Stereochemical Course of Enzymatic Enolpyruvyl Transfer and Catalytic Conformation of the Active Site Revealed by the Crystal Structure of the Fluorinated Analogue of the Reaction Tetrahedral Intermediate Bound to the Active Site of the C115A Mutant of MurA‡

Tadeusz Skarzynski,*,§ Dennis H. Kim,|| Watson J. Lees,|| Christopher T. Walsh,|| and Kenneth Duncan§

Glaxo Wellcome Research and Development, Medicines Research Centre, Stevenage, Hertfordshire, United Kingdom SG1 2NY, and Department of Biological Chemistry and Molecular Pharmacology, Harvard Medical School, Boston, Massachusetts 02115

Received September 10, 1997; Revised Manuscript Received December 5, 1997

ABSTRACT: MurA (UDP-GlcNAc enolpyruvyl transferase), the first enzyme in bacterial peptidoglycan biosynthesis, catalyzes the enolpyruvyl transfer from phosphoenolpyruvate (PEP) to the 3′-OH of UDP-GlcNAc by an addition−elimination mechanism that proceeds through a tetrahedral ketal intermediate. The crystal structure of the Cys115-to-Ala (C115A) mutant of *Escherichia coli* MurA complexed with a fluoro analogue of the tetrahedral intermediate revealed the absolute configuration of the adduct and the stereochemical course of the reaction. The fluorinated adduct was generated in a preincubation of wild-type MurA with (*Z*)-3-fluorophosphoenolpyruvate (FPEP) and UDP-GlcNAc and purified after enzyme denaturation. The fluorine substituent stabilizes the tetrahedral intermediate toward decomposition by a factor of 10^4-10^6, facilitating manipulation of the adduct. The C115A mutant of MurA was utilized to avoid the microheterogeneity that arises in the wild-type MurA from the attack of Cys115 on C-2 of FPEP in competition with the formation of the fluorinated adduct. The crystal structure of the complex was determined to 2.8 Å resolution, and the absolute configuration at C-2 of the adduct was found to be 2*R*. Thus, addition of the 3′-OH of UDP-GlcNAc is to the 2-*si* face of FPEP, corresponding to the 2-*re* face of PEP. Given the previous observation that, in D_2O, the addition of D^+ to C-3 of PEP proceeds from the 2-*si* face [Kim, D. H., Lees, W. J., and Walsh, C. T. (1995) *J. Am. Chem. Soc. 117*, 6380−6381], the addition across the double bond of PEP is anti. Also, because the overall stereochemical course has been shown to be either anti/syn or syn/anti [Lees, W. J., and Walsh, C. T. (1995) *J. Am. Chem. Soc. 117*, 7329−7337], it now follows that the stereochemistry of elimination of H^+ from C-3 and P_i from C-2 of the tetrahedral intermediate of the reaction is syn.

The first committed step in the biosynthetic pathway of the peptidoglycan layer of the bacterial cell wall is the transfer of the enolpyruvyl group of phosphoenolpyruvate (PEP)[1] to the 3′-OH of UDP-GlcNAc, catalyzed by UDP-GlcNAc enolpyruvyl transferase (MurA). This unusual vinyl ether transfer is of the same type as the reaction catalyzed by 5-enolpyruvylshikimate-3-phosphate (EPSP) synthase in aromatic amino acid biosynthesis. MurA is the molecular target of the epoxypropane phosphonate antibiotic, fosfomycin, which inhibits the enzyme by UDP-GlcNAc-dependent alkylation of Cys115 (*1*−*3*). The reaction pathway of *Escherichia coli* MurA has been investigated using rapid-quench kinetics (*4*, *5*), analogues of PEP (*6*−*8*), and site-directed mutagenesis (*9*). From these studies an addition−elimination mechanism for MurA catalysis has emerged (Scheme 1), which proceeds through a tetrahedral intermediate, where C-3 of PEP becomes a methyl group, and C-2 a ketal with phosphate and UDP-GlcNAc substituents. A covalent adduct between PEP and the thiol group of Cys115 has been shown to be off the main catalytic pathway (*7*, *9*). To analyze the mechanism of the tetrahedral adduct formation and breakdown, the nature of the transition states, and the stereochemistry of the addition and elimination steps, substrate analogues such as (*E*)- and (*Z*)-phosphoenolbutyrate (*8*) and (*E*)- and (*Z*)-3-fluorophosphoenolpyruvate (FPEP) were used (*6*, *7*, *10*). The overall stereochemistry of the addition of ROH to PEP and subsequent elimination of H^+

Scheme 1: Addition−Elimination Mechanism for MurA

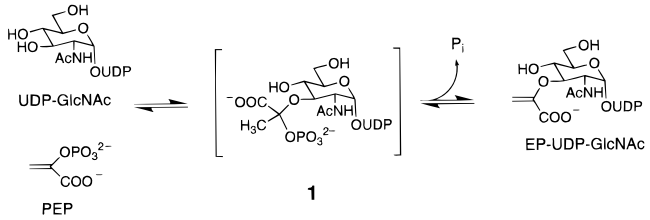

‡ Atomic coordinates have been deposited with the Brookhaven Protein Data Bank, file name 1A2N.

* Author to whom correspondence should be addressed. E-mail: ts14913@ggr.co.uk.

§ Glaxo Wellcome.

|| Harvard Medical School.

[1] Abbreviations: PEP, phosphoenolpyruvate; UDP-GlcNAc, uridine diphospho-*N*-acetyl-D-glucosamine; MurA, UDP-GlcNAc enolpyruvyl transferase; EPSP, 5-enolpyruvylshikimate-3-phosphate; FPEP, 3-fluorophosphoenolpyruvate; C115A, Cys115-to-Ala mutant form of MurA; HPLC, high-performance liquid chromatography.

S0006-2960(97)02260-5 CCC: $15.00
Published on Web 02/04/1998

Scheme 2: Inactivation of MurA by FPEP

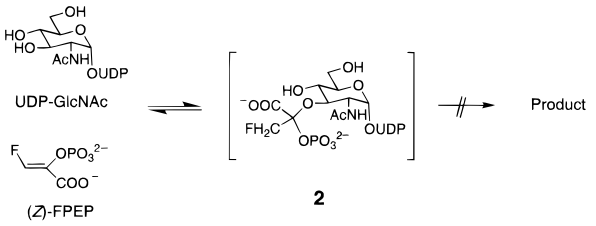

and P_i from the tetrahedral ketal intermediate has been determined by stereochemical analysis of products, containing either an enolbutyryl group or a [^{2}H,^{3}H]enolpyruvyl moiety, to proceed in paired steps that are either anti/syn or syn/anti for both MurA (*8*) and EPSP synthase (*11*, *12*). However, the analysis of the stereochemical outcome at C-2 and C-3 of the ketal intermediate was difficult since the intermediate is formed only transiently and remains bound in the enzyme active site.

Our observation (*6*, *7*) that substitution of PEP by (*E*)- or (*Z*)-FPEP brought MurA to a halt in midcatalytic cycle because the fluoromethyl tetrahedral ketal analogue, **2** (Scheme 2), of the reaction intermediate, **1**, was electronically stabilized some 10^4-10^6-fold and did not decompose to product, allowed the isolation and subsequent characterization of the analogue. When MurA was incubated with FPEP in D_2O and stoichiometric quantities of monodeuterated **2** were released by enzyme denaturation, the chiral CHDF-fluoromethyl group at C-3 was analyzed by ^{1}H NMR, and after enzymatic conversion to 3-fluoromalates the stereochemical assignment could be determined (*10*).

To address the chirality of C-2 in the adduct **2** and by inference, the reaction intermediate **1**, we undertook an X-ray structure determination of **2** complexed with the C115A mutant of MurA. The mutant enzyme was used because in wild-type MurA, the nucleophilic Cys115 attacks PEP and FPEP at C-2 to yield an equilibrating mixture of **1** or **2** and the corresponding covalent *S*-phospholactyl adducts, introducing microheterogeneity that would impede the structure determination. We report the preparation and isolation of **2** from incubations with wild-type MurA, stoichiometric binding of **2** to the Cys115-to-Ala mutant form of MurA (C115A), crystallization of the C115A·**2** complex, solution of the complex structure based on wild-type *E. coli* MurA (*13*), and determination of the structure and chirality of the ketal adduct **2**.

EXPERIMENTAL PROCEDURES

General Materials. MurA and C115A were isolated as described previously (*7*, *14*). The fluorinated adduct **2** (0.5 mg) was prepared from large-scale inactivation reactions of MurA (100 mg of enzyme) with FPEP as described previously (*7*). The ^{14}C analogue of **2** was prepared as described previously (*7*).

Gel Filtration Studies. Size-exclusion HPLC was performed on a SEC-125 (Biorad) column operating at a flow rate of 1 mL/min (50 mM Tris-HCl, pH 7.6). C115A (1 μM) and [^{14}C]**2** (1 and 2 μM) were combined in a total volume of 50 μL of 50 mM Tris-HCl, pH 7.6, and analyzed by size-exclusion HPLC. ^{14}C was detected with an in-line radioisotope detector (Beckman model 171) upon mixing of the eluent with liquid scintillation cocktail (Beckman Ready Flow III) in a ratio of one part eluent to three parts cocktail.

Crystallization. Crystals were grown at 4 °C using the vapor-diffusion sitting-drop method from the solution containing ~9 mg/mL protein and the adduct **2** in a 1:2 ratio (protein to adduct), mixed with an equal volume of the reservoir solution containing 25% *tert*-butyl alcohol, 100 mM $CaCl_2$, and 100 mM Tris-HCl buffer, pH 8.5. Hexagonal rod-shaped crystals of maximum dimensions 100 × 70 × 70 μm were subsequently transferred to a solution of 40% *tert*-butyl alcohol, 100 mM $CaCl_2$, and 100 mM Tris-HCl buffer, pH 8.5. The crystals belong to the trigonal space-group *P*321 with one molecule in the asymmetric unit, and cell dimensions of $a = 111.2$ Å and $c = 67.5$ Å. The crystallization conditions and the crystal cell dimensions are very similar to those for the crystals of native MurA complexed with UDP-GlcNAc and fosfomycin (*13*).

Data Collection and Processing. X-ray diffraction data were collected from a single flash-frozen crystal maintained at 100 K in a stream of dry nitrogen, using the Cryostream system (Oxford Cryosystems), on station 9.6 at the synchrotron radiation source at Daresbury. Data processing was carried out using MOSFLM (*15*) and programs from the CCP4 suite (*16*). The resulting data set was 99.2% complete in the 20−2.8 Å resolution range, with a crystallographic *R*-factor on symmetry-equivalent reflections of 0.108.

Structure Determination. The similarity between the crystal cell dimensions of the MurA·UDP-GlcNAc·fosfomycin complex and the C115A·**2** complex suggested that the structure of the former (*13*) could be used as a starting model in the structure determination of C115A·**2**. The atomic coordinates of the substrate and the inhibitor were removed from the MurA·UDP-GlcNAc·fosfomycin structure, and a crystallographic *R*-factor for the resulting C115A model was 0.35 for all data in the resolution range between 10 and 3.0 Å. Several cycles of least-squares refinement using program PROLSQ (*17*) reduced the *R*-factor to 0.20. A difference electron density computed at this stage clearly showed the outline of the ligand **2** in the enzyme active site. The atomic coordinates of **2** were included in the model, and several model modifications and refinement cycles were carried out using programs QUANTA and X-PLOR (*18*), which resulted in an *R*-factor of 0.175 for all data between 10 and 2.8 Å. The final structure consists of 3129 protein atoms (residues 1−418), 271 water molecules, and the adduct **2**. The stereochemical quality of the structure was checked with the program PROCHECK (*19*), which shows good geometry, with only two residues having the main-chain ϕ/ψ torsion angles in the additional allowed regions of the Ramachandran plot, and no residues in disallowed regions of the diagram. The rms deviation from ideality for bond lengths is 0.02 Å, and for bond angles is 3.4°.

RESULTS

Formation of a 1:1 Complex of C115A MurA and 2. The size-exclusion HPLC analysis, used to determine the stoichiometric composition of the C115A·**2** complex by titration of C115A MurA with [^{14}C]**2**, clearly demonstrated the formation of a 1:1 complex between the enzyme and the fluorinated adduct (Figure 1). No decomposition of **2**, in either forward or reverse directions, was detectable (<2%) over 50 h.

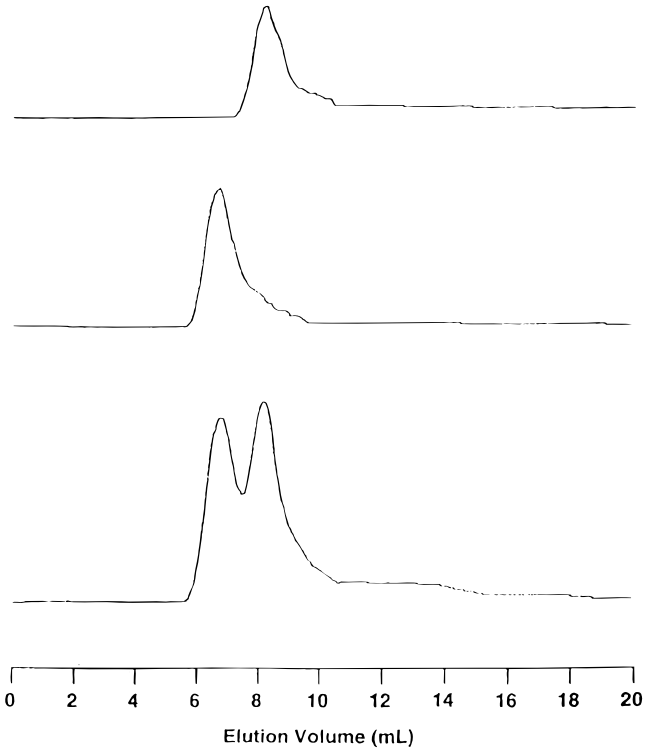

FIGURE 1: Stoichiometric titration of C115A with **2**. Size exclusion HPLC chromatograms of [^{14}C]**2** alone (top), [^{14}C]**2** + C115A MurA (1:1) (middle), and [^{14}C]**2** + C115A MurA (2:1) (bottom).

Overall Structure of the Complex. Since the 1.8 Å resolution structure of the original MurA·DP-GlcNAc·fosfomycin complex was used as a starting model in the refinement of C115A·**2**, the resulting final model for C115A·**2** is of a much higher quality than would be expected from a 2.8 Å resolution structure. The overall protein fold of the C115A·**2** complex is indeed very similar to that of the original MurA·UDP-GlcNAc·fosfomycin complex, with an rms difference of 0.58 Å after the superposition of the main-chain atoms of the two structures (Figure 2). The MurA structure consists of two globular domains connected by a double linker at the bottom of the active site. The internal architecture of both domains is similar, with the "two-α-helix, four-β-strand" motif repeated three times around an approximate 3-fold symmetry axis. The same protein architecture was observed in the structure of the apo form of EPSP synthase (*20*) and the apo form of *Enerobacter cloacae* MurA (*21*). However, the ligand-free structures of EPSP synthase and *Ent. cloacae* MurA are in an "open" conformation, with more space between the domains.

The superposition of the MurA·UDP-GlcNAc·fosfomycin and C115A·**2** structures reveals that only two segments of the polypeptide chain differ significantly: the fragment between residues 82 and 93, with α-carbon positions shifted by up to 1.9 Å (Arg91), and the segment 111−116, including the mutated Ala115, with shifts of up to 6.7 Å (Gly114) (Figure 2). Removal of these two sections from the superposition of the native and mutant complexes results in an rms difference of only 0.35 Å. Atomic temperature factors for residues 111−116 are higher than the temperature factors for neighboring residues and the corresponding electron density less well defined, which suggests some conformational flexibility in this part of the molecule. The two segments of the main chain, 82−93 and 111−116, are close to the tetrahedral intermediate analogue **2**, bound in the active site. The conformational change of these two segments creates an opening in the catalytic pocket near the C-2 tetrahedral center of **2**, and moves the mutated Ala115 (a cysteine in the native enzyme) away from the C-2 substituents. The distance between the fluoromethyl carbon atom bound to C-2 and the α-carbon atom of Ala115 is 10.4 Å.

Protein−Ligand Interactions. The catalytic site of MurA is located in a deep cleft between the two domains. Amino acids from both domains contribute to the binding of **2**

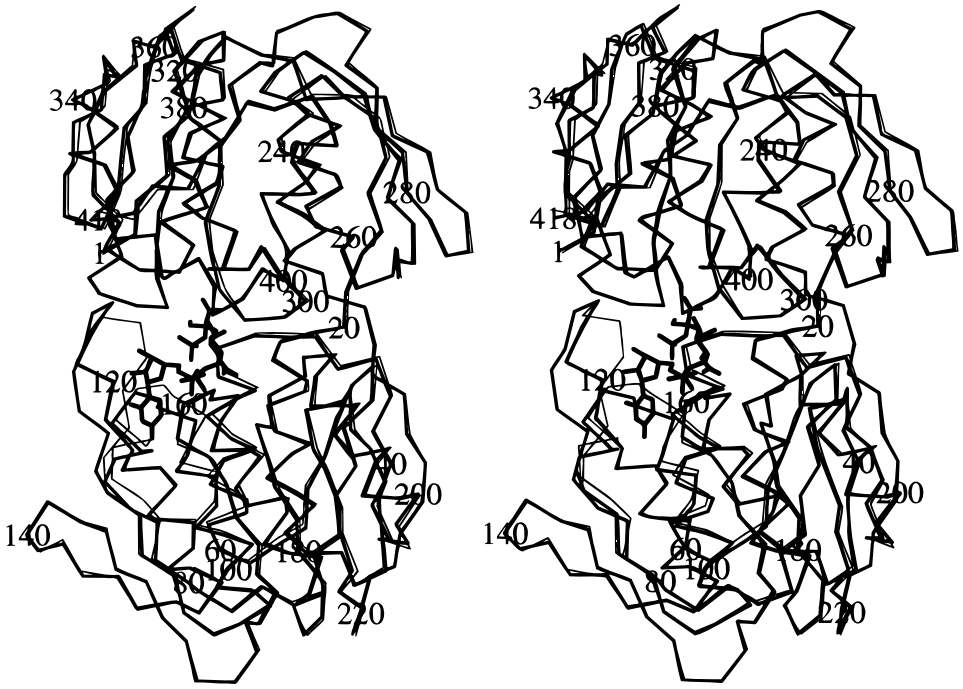

FIGURE 2: Stereoview of the α-carbon backbone of C115A·**2** (thick lines) superimposed on the backbone of MurA·UDP-GlcNAc·fosfomycin complex (thin lines), with the outline of **2** bound in the active site shown as well.

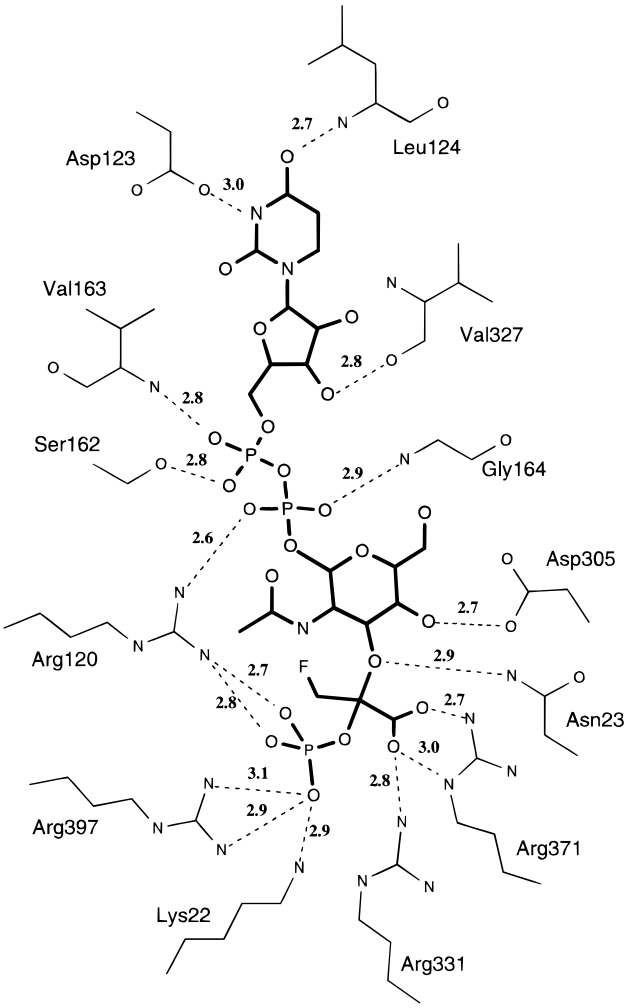

FIGURE 3: Schematic diagram of hydrogen bonds formed between the tetrahedral adduct **2** and the C115A mutant of MurA. Hydrogen bonds are drawn with broken lines.

(Figure 3). The protein−ligand interactions for the uridine and ribose moieties of **2** are identical with those for the substrate UDPGlcNAc in the native MurA·UDP-GlcNAc·fosfomycin complex (*13*). The uridinyl ring of **2** is packed against two hydrophobic patches formed by Arg120 and Pro121 on one side and Leu124 on the other. It also forms hydrogen bonds with Asp123 and Leu124. The ribose moiety forms one hydrogen bond with the main-chain oxygen atom of Val327, while the pyrophosphate bridge is involved in hydrogen bonds with main-chain nitrogen atoms of Val163 and Gly164, the hydroxyl of Ser162, and the guanidinium moiety of Arg120. The hydrogen bond between the pyrophosphate group of **2** and Arg91, observed in the structure of the native complex, is not formed in the present structure due to a different conformation of the Arg91 side chain. The *N*-acetylglucosamine group forms hydrogen bonds with Asn23 and Asp305. However, in contrast to the native complex structure, where two hydrogen bonds were formed with Asp305, only one hydrogen bond is formed with this residue in C115A·**2**.

The interactions between the negatively charged fluorinated tetrahedral ketal group of **2** and the active-site residues involve a lysine and four arginine residues (Figure 3). The phosphate group forms hydrogen bonds with Lys22, Arg120, and Arg397, in a fashion similar to the interactions of the phosphonate group of fosfomycin in the native complex structure. However, the geometry of the interactions is somewhat modified as a result of a different orientation of the phosphate and the phosphonate groups in the two structures. The carboxylate group of the adduct is positioned in a small pocket at the bottom of the active site and forms two hydrogen bonds with Arg371 and one hydrogen bond with Arg331. In the native MurA·UDP-GlcNAc·fosfomycin complex this pocket is occupied by a water molecule. The arginine residue at position 120, conserved in all known MurA and EPSP synthase sequences, interacts with two phosphate groups of **2** (Figure 3) and is the nearest residue to the fluoromethyl carbon atom of the tetrahedral center (3.6 Å). All the other residues in the vicinity are positioned at least 4 Å from the fluoromethyl carbon.

Structure of the Tetrahedral Adduct. Electron density corresponding to the adduct **2** clearly shows the relative arrangement of the fluoromethyl, carboxyl, and phosphate groups around the C-2 atom at the tetrahedral center (Figure 4). This arrangement results in the 2*R* absolute configuration at C-2, which corresponds to the 2*S* configuration for the native reaction intermediate (the presence of the fluorine substituent causes a change in the relative priority of the methyl and carboxylate groups of the adduct). The conformation of the remaining parts of the adduct is very similar to the conformation of UDP-GlcNAc in the complex with fosfomycin-inhibited native enzyme (*13*).

DISCUSSION

Snapshot of the Enzyme−Intermediate Complex. The structure of an enzyme bound to an analogue of the transition state or intermediate provides the most detailed portrait of the catalytic strategies utilized by enzymes because of the critical role that stabilization of the transition state plays in enzymic catalysis. The structure of such high-affinity complexes often also provides a starting point for the design of inhibitors. As is the case with most transient reaction intermediates, the rapid formation and decomposition of the native intermediate **1** precludes structural analysis of **1** at the MurA active site. The stability of the fluorinated tetrahedral adduct **2**, formed at the active site of MurA from FPEP and UDP-GlcNAc, was utilized in kinetic and stereochemical studies of MurA mechanism (*7*, *10*). Thus, **2** would appear to be an ideal candidate for cocrystallization attempts. However, inactivation of wild-type MurA with FPEP results in 1:1 partitioning between **2** and the fluoro analogue of the covalent phospholactyl−enzyme adduct (*7*). It was observed that the catalytically active C115D mutant does not yield the off-pathway covalent phospholactyl adduct, but instead, its inactivation results in an internal equilibrium between the enzyme·UDP-GlcNAc·FPEP ternary complex and the enzyme·**2** complex (*9*). The resulting active site heterogeneity in the case of both catalytically active forms of MurA did not favor crystallization experiments. Consequently, we turned our attention to the analysis of the catalytically inactive C115A mutant, which does not catalyze either the addition or elimination steps in the formation and decomposition of **2** (*22*), while the replacement of Cys115 prevents formation of the covalent phospholactyl adduct. Finally, the C115A active site retains high affinity for **2**, resulting in the formation of a stable 1:1 complex between C115A MurA and **2**. The comparison of the native MurA·

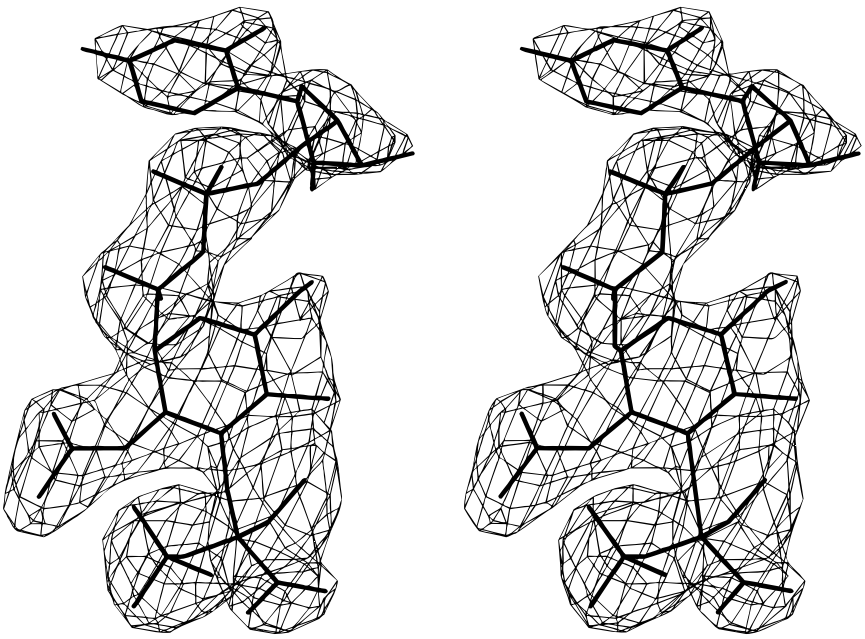

FIGURE 4: Stereoview of electron density corresponding to the tetrahedral adduct **2** (an omit map contoured at 4.0σ).

Scheme 3: Stereochemical Course of Enolpyruvyl Transfer

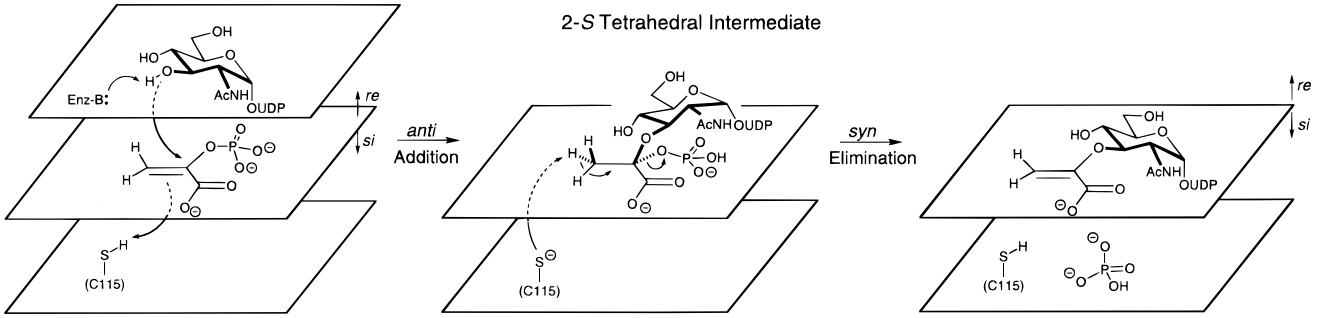

UDP-GlcNAc·fosfomycin structure with that of the mutant C115A·**2** complex reveals close similarity of the active site geometry and the protein−ligand interactions. Therefore, the structure of the C115A·**2** complex provides not only the structure and stereochemistry of the bound tetrahedral adduct **2**, but also a detailed view of a likely catalytic conformation of the MurA active site.

Stereochemical Course of Enzymatic Enolpyruvyl Transfer. The 2*R* configuration of the fluorinated tetrahedral adduct evaluated from the structure determination corresponds to the 2*S* configuration for the native reaction intermediate. Hence, addition of the 3′-OH of UDP-GlcNAc to C-2 of PEP proceeds from the 2-*re* face of PEP. It has been previously established that protonation at C-3 of PEP proceeds from the 2-*si* face of PEP (*10*); thus, addition to the double bond of PEP is anti. Furthermore, based on the constraint on the overall stereochemical course of the reaction in which the addition and elimination steps proceed with opposite stereochemistry (*8*), elimination from the tetrahedral adduct is syn. The stereochemical course of the reaction is illustrated in Scheme 3.

It has been recently determined that the addition at C-3 of PEP in the EPSP synthase reaction also proceeds from the 2-*si* face, and, as an NMR analysis of fluoromethyl hydrogen chemical shifts suggested, the respective tetrahedral adducts from the MurA and EPSP synthase reactions share the same configuration at C-2 (*23*). The chirality of the tetrahedral intermediate at C-2 in the EPSP synthase reaction was a matter of some debate. The inhibition studies of EPSP synthase using diastereomeric phosphonate analogues showed a 70-fold preference for the 2*R* diastereomer, which would indicate an analogous configuration for the native intermediate (*24*). On the other hand, the cyclic ketal side-product of the reaction was suggested to form by SN2 displacement of the 2*S* tetrahedral center of the reaction intermediate (*25*). In view of the results presented in this paper for MurA, we anticipate that the tetrahedral intermediate in the EPSP synthase reaction will also have the 2*S* configuration, and given the same constraint on the overall stereochemical course of the reaction (*11*, *12*), follow the stereochemical course illustrated in Scheme 3 for MurA.

Active Site Stabilization of the Intermediate. The close similarity of this C115A·**2** structure to the recently determined fosfomycin-inactivated MurA structure, and the significant differences between these two structures and the unliganded MurA structure (*21*), support previous biochemical studies (*1*−*3*) which found that the binding of UDP-GlcNAc induces a conformational change in the enzyme with fosfomycin acting as an analogue of PEP, mimicking both the chemistry and structure of the native substrate. The phosphate of the tetrahedral adduct is involved in interactions with the same residues as the phosphonate group of fosfo-

mycin (Figure 3). As anticipated from modeling studies, based on the fosfomycin-inactivated MurA structure (T. Skarzynski, unpublished results), the carboxylate group of the tetrahedral adduct makes contacts with two conserved arginine residues: Arg381 and Arg331. The structure-based alignment of the MurA and EPSP synthase sequences indicates a similar carboxylate-binding arrangement in EPSP synthase.

Role of the Cys115 Loop in Catalysis. Recent mutagenesis studies have indicated that residue 115 is involved in general acid−base catalysis (*9*). In the fosfomycin-inactivated MurA structure, Cys115 appears to be positioned to carry out general acid−base catalysis, but this interpretation is complicated by the alkylation of the thiol side chain. However, assuming that fosfomycin acts as an analogue of PEP, the observed conformation of the Cys115 loop in the MurA·UDP-GlcNAc·fosfomycin structure places the side chain of residue 115 in an appropriate position to carry out the first (addition) stage of the reaction, leading to the formation of the tetrahedral ketal intermediate **1**. Our modeling studies, in which we replaced fosfomycin with noncovalently bound PEP, show that the 3′ hydroxyl of UDP-GlcNAc and Cys115 are oriented anti with respect to the modeled PEP, with Cys115 situated on the 2-*si* face (T. Skarzynski, unpublished results).

The Cys115 loop, anchored by proline residues (Pro112 and Pro121) and containing three glycine residues (Gly113, Gly114, and Gly118), seems to be very flexible. In the nonliganded *Ent. cloacae* MurA (*21*) Cys115 is exposed to solvent, and is situated far from the active site cleft. In the structure of *E. coli* C115A·**2**, presented here, the conformation of this loop is different from that observed in *Ent. cloacae* MurA, but it also differs from the conformation in the MurA·UDP-GlcNAc·fosfomycin complex. The crystal environment of the two *E. coli* structures is virtually identical, with no direct interactions between the Cys115 loop and symmetry-related protein molecules. Therefore, the observed conformational differences cannot be simply attributed to crystal forces. It is likely that the three known MurA structures correspond to three different stages of the enzyme catalysis: prior to the reaction (nonliganded *Ent. cloacae* MurA), just before the addition reaction leading to the formation of the tetrahedral adduct **1** (fosfomycin-inactivated *E. coli* MurA), and just before the proton transfer and elimination of inorganic phosphate (*E. coli* C115A·**2**). The conformational change of the Cys115 loop in the C115A·**2** structure and positional shifts of several residues in this region, which result in the partial opening of the active-site pocket, would allow inorganic phosphate to leave the active site in the final step of the reaction. For example, the positional shift and conformational change of Arg91 alter its interaction with the pyrophosphate bridge of the ligand and seem to create a new phosphate-binding site situated next to the phosphate group of **2**, as indicated by our modeling calculations. In comparison with the fosfomycin-inactivated *E. coli* MurA structure, the salt bridge Asp49−Arg397 is weakened, as is the interaction between the ligand and Asp305 from the C-terminal domain. This is also consistent with the expected structural changes in the active site required for the next step of reaction.

For Cys115 to function as proton-transfer catalyst, as suggested in Scheme 3, the 112−121 loop must rearrange to take up a position similar to that seen in the fosfomycin-inactivated wild-type enzyme. Although previous data (*7*, *9*, *10*, *23*) indicate that Cys115 is essential for decomposition of tetrahedral intermediate **1** in both forward and backward directions, it is possible that this residue is not the direct proton-transfer agent to and from C-3 of PEP and **1**. For example, one of the phosphate oxygen atoms is only 2.5 Å from the C-3 carbon atom of the fluoromethyl group of **2** (Figure 3) and could act as an intramolecular proton-transfer agent.

REFERENCES

1. Kahan, F. M., Kahan, J. S., Cassidy, P. J., and Kropp, H. (1974) *Ann. N.Y. Acad. Sci. 235*, 364−386.
2. Wanke, C., and Amrhein, N. (1993) *Eur. J. Biochem. 218*, 861−870.
3. Marquardt, J. L., Brown, E. D., Lane, W. S., Haley, T. M., Ichikawa, Y., Wong, C.-H., and Walsh, C. T. (1994) *Biochemistry 33*, 10646−10651.
4. Marquardt, J. L., Brown, E. D., Walsh, C. T., and Anderson, K. S. (1993) *J. Am. Chem. Soc. 115*, 10398−10399.
5. Brown, E. D., Marquardt, J. L., Lee, J. P., Walsh, C. T., and Anderson, K. S. (1994) *Biochemistry 33*, 10638−10645.
6. Kim, D. H., Lees, W. J., and Walsh, C. T. (1994) *J. Am. Chem. Soc. 116*, 6478−6479.
7. Kim, D. H., Lees, W. J., Haley, T. M., and Walsh, C. T. (1995) *J. Am. Chem. Soc. 117*, 1494−1502.
8. Lees, W. J., and Walsh, C. T. (1995) *J. Am. Chem. Soc. 117*, 7329−7337.
9. Kim, D. H., Lees, W. J., Kempsell, K. E., Lane, W. S., Duncan, K., and Walsh, C. T. (1996) *Biochemistry 35*, 4923−4928.
10. Kim, D. H., Lees, W. J., and Walsh, C. T. (1995) *J. Am. Chem. Soc. 117*, 6380−6381.
11. Grimshaw, C. E., Sogo, S. G., Copley, S. D., and Knowles, J. R. (1984) *J. Am. Chem. Soc. 106*, 2699−2700.
12. Lee, J. J., Asano, Y., Shieh, T.-L., Spreafico, F., Lee, K., and Floss, H. G. (1984) *J. Am. Chem. Soc. 106*, 3367−3368.
13. Skarzynski, T., Mistry, A., Wonacott, A., Hutchinson, S. E., Kelly, V. A., and Duncan, K. (1996) *Structure 4*,1465−1474.
14. Marquardt, J. L. (1993) Ph.D. Thesis, Harvard University, Boston, MA.
15. Leslie, A. G. W., Brick, P., and Wonacott, A. J. (1986) MOSFLM, *Daresbury Lab. Inf. Q. Protein Crystallogr. 18*, 33−39.
16. Collaborative Computational Project, No. 4 (1994) The CCP4 Suite: Programs for protein crystallography, *Acta Crystallogr. D50*, 760−763.
17. Hendrickson, W. A., (1985) *Methods Enzymol. 115*, 252−271.
18. Brünger, A. T., Kuriyan, J., and Karplus, M. (1987) *Science 235*, 458−460.
19. Laskowski, R. A., MacArthur, M. W., Moss, D. S., and Thornton, J. M. (1993) *J. Appl. Crystallogr. 26*, 283−291.
20. Stallings, W. C., Abdel-Meguid, S. S., Lim, L. W., Shieh, H.-S., Dayringer, H. E., Leimgruber, N. K., Stageman, R. A., Anderson, K. S., Sikorski, J. A., Padgette, S. R., and Kishore, G. M. (1991) *Proc. Natl. Acad. Sci. U.S.A. 88*, 5046−5050.
21. Schönbrunn, E., Sack S., Eschenburg, S., Perrakis, A., Krekel, F., Amrhein, N., and Mandelkow, E. (1996) *Structure 4*, 1065−1075.
22. Kim, D. H. (1996) Ph.D. Thesis, Harvard University, Boston, MA.
23. Kim, D. H., Tucker-Kellogg, G. W., Lees, W. J., and Walsh, C. T. (1996) *Biochemistry 35*, 5435−5440.
24. Alberg, D. G., and Bartlett, P. A. (1989) *J. Am. Chem. Soc. 111*, 2337−2338.
25. Leo, G. C., Sikorski, J. A., and Sammons, R. D. (1990) *J. Am. Chem. Soc. 112*, 1653−1654.

BI9722608